

Superconductivity of 80NbN–20SiO₂ granular films

O. I. Yuzepovich^{a)} and S. V. Bengus

B. I. Verkin Institute of Low Temperature Physics and Engineering, pr. Lenina 47, Kharkiv 61103, Ukraine and International Laboratory of High Magnetic Fields and Low Temperatures, 53-421 Wrocław, Poland

B. Kościelska and A. Witkowska

Faculty of Applied Physics and Mathematics, Gdańsk University of Technology, 080-952 Gdańsk, Poland

(Submitted April 19, 2010)

Fiz. Nizk. Temp. **36**, 1312–1319 (December 2010)

The feasibility of creating granular superconducting films of NbN–SiO₂ with a controlled grain size by a sol-gel method is demonstrated. A comprehensive study is made of the structural and transport properties of granular films of 80%NbN–20%SiO₂ with different thicknesses. It is found that production of a complete superconducting transition requires that the samples have thicknesses greater than 750 nm. The critical temperatures for a superconducting transition and the upper critical magnetic fields are roughly constant for films with different thicknesses and equal 4.5 K and 4.4 T, respectively. A crossover from 2D to 3D behavior is discovered in the temperature variation of the upper parallel critical field. It is shown that at low magnetic fields the resistive transitions obey an Arrhenius law. The mechanism for broadening of resistive transitions in magnetic fields is most likely magnetic flux creep. The magnetic field dependence of the activation energy is obtained. Typical initial signs of a magnetically induced superconductor-insulator transition are observed at high magnetic fields. © 2010 American Institute of Physics. [doi:10.1063/1.3533238]

I. INTRODUCTION

Research on low dimensionality systems, such as ultrathin films, nanodispersed granular systems, quantum dots, quantum bits, etc., has recently been expanding rapidly. These systems have fundamentally new, unique properties and manifest unusual quantum mechanical effects. Chemically and physically stable materials are required for the development, creation, and utilization of nanostructured systems with specified properties and new functional capabilities. With its high adhesion and durability,^{1,2} chemical inertness,^{3,4} stability under thermal cycling,⁵ and high melting point, NbN has properties of this sort and is one of the priority materials for microelectronics. Its superconducting properties are of particular interest and include a high critical temperature (up to 17 K for the bulk material) and high critical magnetic fields and critical currents (for thin films $J_c \sim 10^7$ A/cm²). A short coherence length $\xi = 4\text{--}7$ nm and a long London magnetic field penetration depth $\lambda_{\text{NbN}} = 180$ nm are observed in thin films. Ultrathin, homogeneous NbN films are widely used to make superconducting detectors, filters, single-photon transistors, and antennas.^{6–8}

The structural and electrical properties of NbN films depend very strongly on the fabrication techniques. Introducing disorder into a film leads, on one hand, to a reduction in the critical temperature while, on the other, it may increase such parameters as the critical current and critical magnetic field. In addition, disorder is one of the possible mechanisms responsible for the appearance of quantum mechanical effects such as a superconductor-insulator transition,^{9–13} stochastic resonance,^{14,15} etc. Thus, from a basic, as well as applied, standpoint, there is some interest in the feasibility of creating

granular structures with specified NbN grain sizes in insulating matrices. Granular films can consist of granules with sizes ranging from a few to hundreds of nanometers and belong to a class of artificial material whose electronic properties are easily modelled.⁹ By fine tuning the coupling between granules a system can be shifted from a “good metal” or superconducting state to an “insulating” state. Superconductivity evolves in stepwise fashion in them; at first individual granules enter a superconducting state and then Josephson couplings develop between them and a global superconducting state of the entire system as a whole sets in.

Thermal vaporization and magnetron sputtering are widely used conventional methods of preparing granular materials. Here we propose an alternative technology which has recently been under rapid development: a sol-gel method for creating granular films with subsequent thermal nitriding. This technology makes it possible to synthesize high quality coatings that meet the strict specifications of modern engineering and to control the size of the superconducting granules in an insulating matrix.¹⁶

In this paper we present the results of a comprehensive study of the structural and superconducting properties of granular films of $x\text{NbN}-(100-x)\text{SiO}_2$ (where $x=80$ mol%) with thicknesses ranging from 450 to 1950 nm. The effect of magnetic fields on the features of the superconducting state is examined and typical signs of magnetic-field induced superconducting-insulator transitions are discovered.

II. EXPERIMENTAL TECHNIQUE

A. Sample preparation and structural characteristics

Films of $x\text{Nb}_2\text{O}_5-(100-x)\text{SiO}_2$ (where $x=10, 80, 60, 50, 40, 20, 0$ mol%) with different thicknesses were prepared by

a sol-gel technique. The initial solution of $x\text{Nb}_2\text{O}_5-(100-x)\text{SiO}_2$ is a mixture of tetraethoxy silane (TEOS, Fluka) and niobium chloride (NbCl_5 , Aldrich) with ethanol and acetyl acetone as a complexing agent. The solution was deposited on a quartz substrate by centrifuging. Substrates with the deposited film were dried for 24 h at room temperature and then in a muffle furnace at 250 °C for about an hour. This procedure yields a film with a thickness of about 150 nm. Thicker films were obtained by repeating this procedure for the required number of times.

After a coating of $x\text{Nb}_2\text{O}_5-(100-x)\text{SiO}_2$ was obtained, the film was subjected to thermal nitriding in a flow-through ammonia medium heated at a rate of 1 °C/min up to a certain temperature and then isothermally for an hour.

Comprehensive structural studies were conducted of samples nitrided at different temperatures. X-ray structural analyses of the films were done on a Philips X'Pert diffractometer in a θ - 2θ geometry using $\text{CuK}\alpha$ radiation. X-ray diffraction patterns were recorded at room temperature before and after the films were nitrided. The SiO_2 phase remains amorphous for any nitriding temperature. With nitriding at 1200 °C, only the crystalline phase of NbN is present in the film, while at lower nitriding temperatures peaks corresponding to crystalline NbO and Nb_2O_5 phases were also observed. Thus, the optimal nitriding temperature was found to be 1200 °C.

Topographic images of all the test samples before and after nitriding were obtained with an atomic force microscope (AFM) on an MSS-system stand (Łódź University, Poland). Some typical AFM topographic images of samples of $x\text{Nb}_2\text{O}_5-(100-x)\text{SiO}_2$ (with $x=80$ and 60 mol%) after nitriding at $T=1200$ °C are shown in Fig. 1. In all of the films, except the pure SiO_2 films, there is a regular nanocrystalline structure and the position of the NbN granules becomes more regular as the amount of niobium is increased. The maximum size of the NbN granules is 100 nm at the maximum concentration $x=100$ mol% (see Table I), although the size of the Nb_2O_3 granules prior to nitriding may reach 500 nm. Thus, varying the molar ratio $\text{Nb}_2\text{O}_5:\text{SiO}_2$ in the initial gel and the nitriding process, together, make it possible to produce NbN- SiO_2 films with specified NbN granule sizes.

The fabrication technique and structural characteristics of the granular NbN- SiO_2 films are described in more detail elsewhere.²

For the studies of the superconducting properties reported here we chose films of $x\text{Nb}_2\text{O}_5-(100-x)\text{SiO}_2$ with $x=80$ mol% and different thicknesses d : 450, 750, 1050, 1350, 1650, and 1950 nm.

B. Transport measurement techniques

Transport measurements were made in a standard Oxford Instruments cryostat equipped with a superconducting solenoid that produced a maximum magnetic field of 14 T and temperatures of 1.4–300 K. The accuracy of the temperature measurement and stabilization over 1.4–10 K was better than 10^{-3} K and over 10–300 K, 0.05 K.

The resistance R was measured by the four-probe method; the samples were in the form of double Hall crosses. Dc and ac (50 nA, 13 Hz) measurements were made. The transport current I was parallel to the plane of the film with

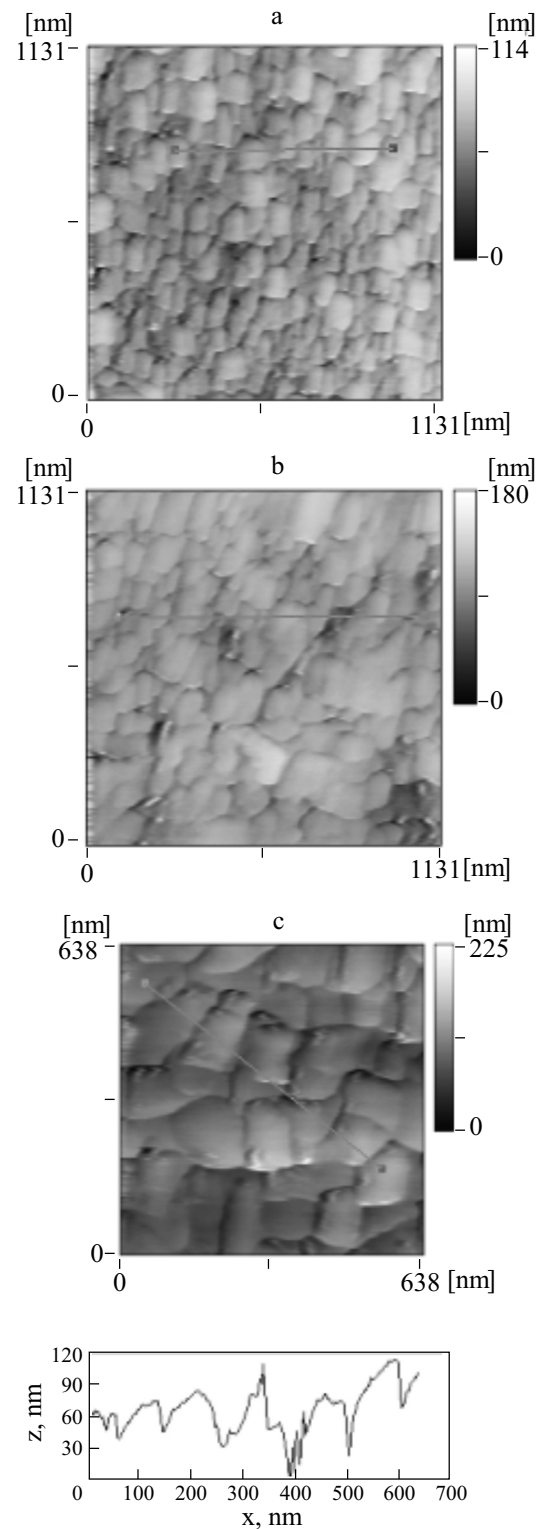


FIG. 1. AFM topographic images of $x\text{Nb}_2\text{O}_5-(100-x)\text{SiO}_2$ films after nitriding: $x=60$ (a), 80 (b), and 100 mol.% (c). The maximum size of the crystallites is 100 nm.

$I \perp H$. The critical magnetic fields H_{c2} were determined from the average of the resistive transitions.

III. EXPERIMENTAL RESULTS AND DISCUSSION

A. Transitions into a superconducting state at $H=0$

Figure 2 shows the temperature variations of the resistance per square for films with thicknesses $d=450, 750,$

TABLE I. Average diameter of NbN granules in a SiO₂ matrix for films with different concentrations of Nb₂O₅ in the starting solution derived from AFM topological images of the films.

Concentration of Nb ₂ O ₅ , mol. %	Average diameter of NbN granules, nm
50	35
60	50
70	60
80	83
100	100

1050, 1350, 1650, and 1950 nm. All the samples had a negative temperature coefficient of resistivity before their superconducting transition and, as can be seen from the inset to Fig. 2, the conductivity has a logarithmic dependence, $\sigma(T) = a + b \ln T$, in agreement with theoretical predictions⁹ for granular metals. A similar type of conductivity has been observed in granular NbN films with smaller granules and in three-dimensional granular systems.^{9,12} No superconducting transition was observed in the 450-nm-thick sample (over temperatures from 300 to 1.4 K). Samples with thicknesses of 750 nm and greater have a superconducting transition. The critical temperatures for the onset of a superconducting transition $T_{c \text{ onset}}$ in zero magnetic field vary somewhat around 8 K, with a slight tendency to increase for thicker films. (See the inset to Fig. 2.) The slight difference in $T_{c \text{ onset}}$ for samples with different thicknesses may be related to the presence of a small amount of crystalline N₂O₅ in the samples.

The critical superconducting transition temperatures T_c determined from the midpoint of the resistive transition at the level of $\rho_{\text{max}}/2$ are equal (as they should be for granular films⁹) and are on the order of 4.5 K.

Figure 3 illustrates the transition to the superconducting state for a film with $d=1350$ nm in zero magnetic field $H=0$ T. The critical temperature for the onset of the transition is $T_c(0.9)=6.39$ K, for the end of the transition, $T_c(0.1)$

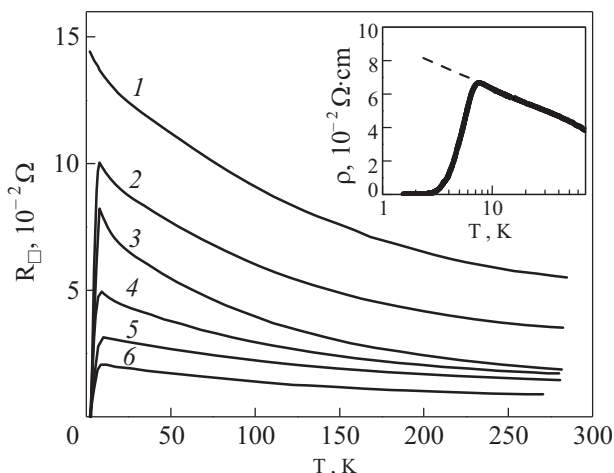


FIG. 2. Temperature variations of the resistance per square for $x\text{Nb}_2\text{O}_5-(100-x)\text{SiO}_2$ films of different thickness: 450 (1), 750 (2), 1050 (3), 1350 (4), 1650 (5), and 1950 nm (6). The inset shows the temperature dependence of the specific resistance for the sample with thickness $d=1350$ nm.

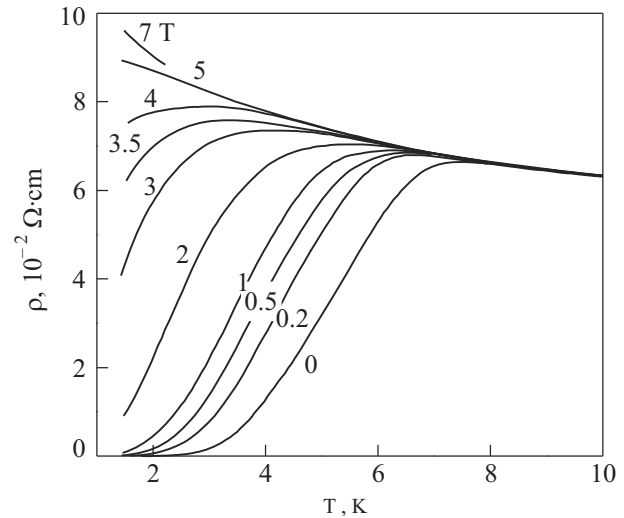


FIG. 3. Temperature dependences of the specific resistance for different values of the perpendicular magnetic field for the sample with thickness $d=1350$ nm.

$=3.59$ K, and for the middle, $T_c(0.5)=4.5$ K. The width is $\Delta T_c = \Delta T(T_{0.9} - T_{0.1}) = 2.8$ K and $T_{c \text{ onset}} \sim 7.5$ K. Global superconducting coherence is established in the system at fairly low temperatures because of the increased Josephson coupling energy between granules. The onset of the superconducting transition is determined by the appearance of superconductivity in the volume of the granules, and the end, by the appearance of superconductivity along weak intergranule paths. The critical temperature of pure NbN is on the order of 16 K (for thin homogeneous films, about 10 K), and for our granular films the critical temperature is a factor of two lower. We may ask, why is there such a large drop in the critical temperature? We cannot provide a unique answer, but this property is not unusual for granular systems. Disorder can significantly reduce the critical temperature. In an ideal system of granules, phase coherence sets in simultaneously over the entire volume, while smearing out of the superconducting transition is controlled by fluctuations in the order parameter. Real systems have a spatial inhomogeneity, both in the granule sizes and in the thicknesses of the dielectric spacers. Percolation models of conduction are more suitable for systems of this kind. According to these theories phase coherence is established only within a limited number of clusters when the temperature is lowered. As the temperature is reduced, the superconducting clusters grow and an infinite cluster develops—the resistance drops to zero.¹⁰ Thus, the large spread in the superconducting transition in zero magnetic field which we have observed may be related to the strong disorder and granularity of the films.

B. Effect of a low magnetic field on the superconducting state

Many systems (granular films, HTSC, films and crystals of MgB₂) manifest a broadening of resistive transitions in low magnetic fields that has been the subject of numerous interpretations and controversies. This phenomenon may be related to structural inhomogeneity, or to fluctuations or creep in the magnetic flux. It is not always easy to distinguish these mechanisms. Figure 3 shows the temperature de-

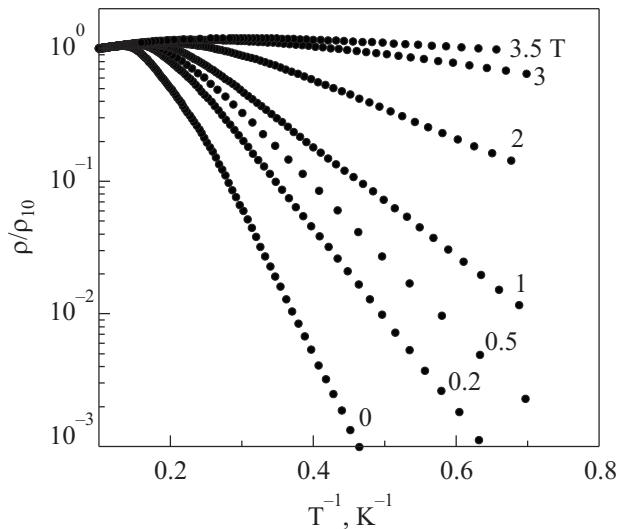


FIG. 4. Normalized resistance as a function of reciprocal temperature for different values of the magnetic field for the sample with thickness $d = 1350$ nm.

pendences of the specific resistance of a film of thickness $d = 1350$ nm for different magnetic fields H perpendicular to the plane of the film. In low magnetic fields the resistive transitions are broadened. The width ΔT of the resistive transition, defined as the difference between the temperatures measured at $0.1\rho_{\max}$ and $0.9\rho_{\max}$, is on the order of 2.8 K in zero magnetic field, while the spreading of the resistive transition is greater, more than 3 K, in a magnetic field of 1.5 T.

The spreading out of the resistive transitions in magnetic fields observed in granular films, HTSC, artificial superlattices, and other inhomogeneous systems has been interpreted in terms of energy dissipation. In our case, the dissipation mechanism is probably associated with magnetic flux creep, since the size of the superconducting granules is considerably greater than the coherence length. This interpretation is justified by the fact that at low resistances ($\rho \ll \rho_{\max}$) the $\rho(T)$ curves have a thermally activated character. In general, this kind of dependence can be written as

$$R = R_0 \exp(-U(H, T)/kT), \quad (1)$$

where $U(H, T)$ is the activation energy, which depends differently on the temperature and magnetic field in different types of structures and k is the Boltzmann constant.^{17,18} ρ is plotted as a function of $1/T$ for a film with $d = 1350$ nm for several values of the magnetic field in Fig. 4. Figure 4, together with the analogous data for other samples, implies that the resistive behavior is well described by an Arrhenius law (1). According to the Anderson and Kim models,¹⁸ the activation energy for magnetic flux creep as a function of magnetic field and temperature can be written in the form $U(H) = U_0 H^\alpha (1 - T/T_c)^\beta$. The activation energy for the film with $d = 1350$ nm is plotted in Fig. 5 as a function of magnetic field. The activation energy in zero magnetic field, $U_0(H = 0)$, is of order 10 K. The variation in the activation energy is characterized by two power laws, with $\alpha = -1/3$ for low fields and shifting to $\alpha = -4$.

The broadening of resistive transitions in granular films for low magnetic fields can also be explained in terms of a model of coupled Josephson junctions. Then the effect is

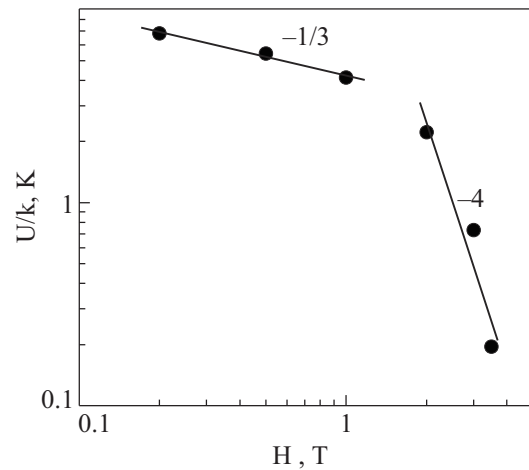


FIG. 5. The activation energy for magnetic flux creep as a function of magnetic field for the sample with thickness $d = 1350$ nm.

independent of the macroscopic Lorentz force, i.e., of the direction of the transport current relative to the magnetic field. This sort of effect has been observed experimentally in granular NbN films.¹⁹ Additional experimental studies are needed in order to compare our results with the theoretical model considered here.

C. Effect of high magnetic fields on the superconducting state

All the initial signs of a magnetically induced superconductor-insulator transition are observed in a sample with $d = 1350$ nm at high magnetic fields. Superconductor-insulator transitions have recently been much studied and experimentally observed in various systems, such as ultrathin amorphous films of $\text{Mo}_x\text{Ge}_{1-x}$, $\text{Mo}_x\text{Si}_{1-x}$, InO_x , Be, Bi, Ta, Bi/Sb, $\text{Nb}_{0.15}\text{Si}_{0.85}$, films of $\text{Nd}_{2-x}\text{Ce}_x\text{CuO}_{4+y}$, granular films, and arrays of Josephson junctions.¹¹ Although a wide range of different low-dimensional systems which manifest superconductor-insulator transitions is already known, the nature of these transitions is not conclusively understood. The phase transition for many structures is explained by the Fisher scaling theory²⁰ (a theory of duality between Cooper pairs and vortices). It is assumed that at $T = 0$ there are delocalized Cooper pairs and localized vortices below the transition, at fields $H < H_c$ (superconductor), and localized pairs on delocalized vortices above the transition $H > H_c$ (insulator). For disordered uniform films with relatively low resistance per square, this effect can be explained by quantum mechanical corrections to the conductivity.²¹ In granular systems with small granule sizes (this model can scarcely apply to our granular films because of the large size of the granules, on the order of 80 nm) the transition is explained by a competition between the Josephson intergranule coupling force and the charge Coulomb energy of individual granules. If the Coulomb blocking has the advantage, the Cooper pairs become localized as $T \rightarrow 0$ and the system undergoes a transition to the insulating state.⁹⁻¹¹ The nature of this fairly universal phenomenon is still not unambiguously understood.

The first sign of a superconductor-insulator transition is a fan-like dependence of the resistance on temperature for different values of the magnetic field. There are three ways the $R(T)$ curves can evolve as the magnetic field is varied.

The first type of curve is fan-like $R(T)$ curves for different values of the magnetic field with a horizontal separatrix separating the families of curves with a superconducting transition from those for which there is no transition. The second type are also fan-like curves, but with an inclined separatrix that tends to steepen or even go to infinity as the temperature is reduced. And the third type—if the fields are sufficiently great, then the first derivative is negative everywhere and in the range of intermediate fields the $R(T)$ curves have two extrema, a minimum near $T_{c\text{ onset}}$ and a maximum at lower temperatures followed by a transition into a superconducting state. A horizontal separatrix is considered to be the ideal case. An inclination of the separatrix may be associated with single particle transport between superconducting granules.¹¹ On the other hand, a minimum of the resistance is observed in systems with very thick dielectric spacers where superconductivity develops in stages—first in the granules and then a Josephson junction develops between them.¹⁰ In our granular films we observe an initial segment of fan-like temperature dependences $\rho(T)$ for the specific resistance with an inclined separatrix (see Fig. 3). Because of the inclined and, apparently, even nonlinear separatrix, it is not possible to use the single-parameter Fisher scaling theory²⁰ and determine the critical resistance R_c of the superconductor-insulator transition. Earlier it was assumed that the superconductor-insulator phase transition is characterized by a universal quantum resistance $R_c \approx h/4e^2 \approx 6.5 \text{ k}\Omega$. Now, relying on many experiments, it is assumed that there is no such universal resistance R_c for these kinds of systems.¹¹ Several interesting arise: is there a special resistance R_c associated with a quantum phase transition; how does it depend on the properties of the corresponding quantum boundary state; and, is it possible to control R_c ? It has been shown with percolation models for superconductor-insulator transitions that the critical resistance depends on the disorder distribution and on the nature of the percolation current channels.²²

The second sign of a magnetically induced superconductor-insulator transition is crossing of the magnetic field dependences of the resistance for different temperatures and the third is negative magnetoresistance in strong magnetic fields (see Fig. 6). Initial signs of a superconductor-insulator transition are observed in the sample with thickness $d=1350 \text{ nm}$ for both parallel and perpendicular magnetic fields. It should be noted that all the characteristic features of a superconductor-insulator transition have appeared at temperatures above 1.4 K and the effect will be more marked at lower temperatures. A detailed experimental study of the features of the superconductor-insulator transitions and a comparison with theoretical models will be carried out later.

D. Upper critical magnetic fields

The variations in the parallel and perpendicular upper critical magnetic fields with temperature for a film with $d=1650 \text{ nm}$ are plotted in Fig. 7. The upper perpendicular and parallel fields at $T=0 \text{ K}$ determined by extrapolating the linear segments of the $H_c(T)$ curves for films with $d=750\text{--}1950 \text{ nm}$ are roughly equal at 4.4 T. Thus, the anisotropy parameter $\gamma=(dH_{c\parallel}/dT)/(dH_{c\perp}/dT)$ for these granular films equals 1. The Ginzburg–Landau theory for classical

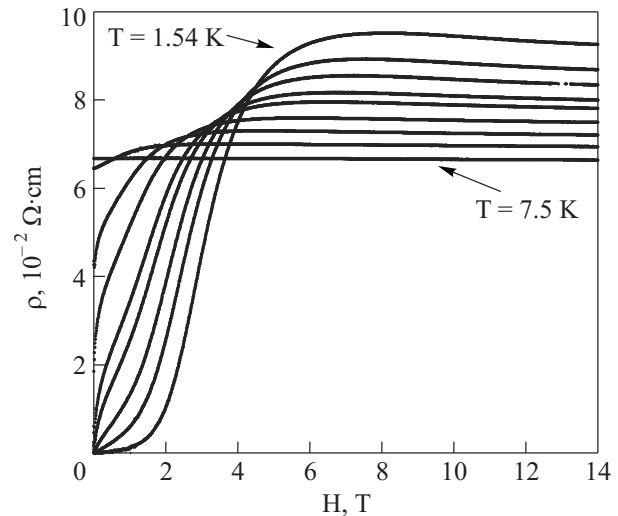


FIG. 6. Specific resistance as a function of magnetic field at temperatures of 1.54, 2.11, 2.53, 3.09, 3.46, 4.19, 5.6, and 7.5 K, for the sample with thickness $d=1350 \text{ nm}$.

type II superconductors, which is valid near T_c , yields the following relationship between the coherence length $\xi(T)$ of a superconducting condensate and the upper critical magnetic field: $H_{c2\perp}(T) = \phi_0/2\pi\xi_{\parallel}^2(T)$, where $\phi_0=2.07 \cdot 10^{-15} \text{ T/m}^2$ is the quantum of magnetic flux. The temperature dependence $H_{c2\perp}(T)$ is linear. According to the Ginzburg–Landau theory, H_{c2} increases as the coherence length decreases; this is related to a reduction in the vortex size. The parallel coherence length $\xi_{\parallel}(0)$ at $T=0$, determined from the perpendicular critical field, is roughly 8 nm.

Figure 7 shows that the perpendicular upper critical field has a linear dependence $H_{c\perp} \sim (T_c - T)$, i.e., the film has 3D behavior. The variation in $H_{c\parallel}$ is close to a square root form (2D behavior) near the transition temperature T_c , but is linear at low temperatures; that is, a 2D-3D crossover is observed

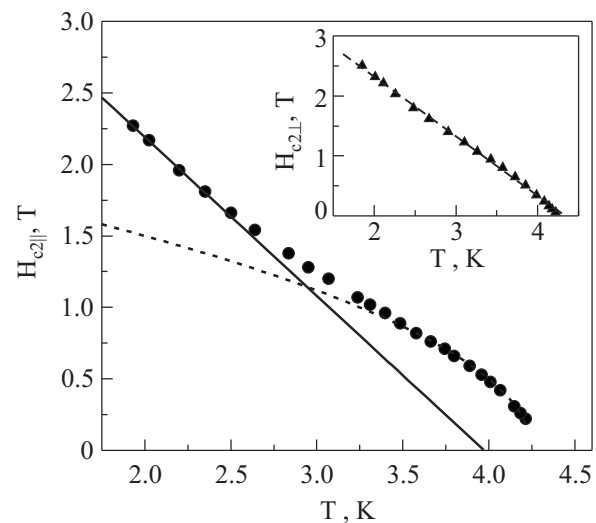


FIG. 7. Temperature dependences of the upper critical magnetic fields for the sample with thickness $d=1350 \text{ nm}$.

(Fig. 7). This crossover can be explained in terms of the Ginzburg–Landau theory and is related to the behavior of a vortex system. This is so, because, on one hand, near T_c the coherence length is comparable to the granule size. On the other hand, the coherence length depends on temperature and decreases with falling temperature; that is, a dimensional crossover is observed in the vortex system.

IV. CONCLUSIONS

1. A sol-gel technique for fabricating granular NbN–SiO₂ films with specified granule sizes has been developed and perfected. The optimum nitriding temperature has been chosen.

2. The critical superconducting transition temperatures (about 4.5 K) and upper critical parallel and perpendicular magnetic fields (4.4 T) have been determined for 80%NbN–20%SiO₂ films with different thicknesses. A 2D to 3D dimensional crossover in the temperature dependence of the upper critical parallel magnetic field has been discovered.

3. It has been found that at low magnetic fields the resistive transitions are well described by an Arrhenius law. The dependence of the activation energy on the magnetic field obeys a power law $U \propto H^{-1/3}$ for low fields and changes to $U \propto H^{-4}$ as the magnetic field is increased. We believe that the most likely mechanism for the broadening of the resistive transitions in low magnetic fields is magnetic flux creep.

4. Initial signs typical of magnetically induced superconductor-insulator phase transitions are observed at high magnetic fields.

This work was supported by a grant from the National Academy of Sciences of Ukraine for young scientists entitled “Magnetic field induced phase transitions in magnetic and nonmagnetic nanostructures” (grant No. 15-2009) and the targeted comprehensive program for basic research of the National Academy of Sciences of Ukraine entitled “Fundamental problems in nanostructured systems, nanomaterials, and nanotechnologies” (grant No. 26/10-N).

^{a)}Email: yuzepovich@ilt.kharkov.ua

-
- ¹V. N. Zhitomirsky, I. Grimberg, L. Rapoport, N. A. Travitzky, R. L. Boxman, and S. Goldsmith, *Thin Solid Films* **326**, 134 (1998).
²B. Kościelska and A. Winiarski, *J. Non-Cryst. Solids* **354**, 4349 (2008).
³M. Larsson, P. Hollman, P. Hendequist, S. Hogmark, U. Wahlstrom, and L. Hultman, *Surf. Coat. Technol.* **86/87**, 351 (1996).
⁴K. Baba, R. Hatada, K. Udoh, and K. Yasuda, *Nucl. Instrum. Methods Phys. Res.* **B127**, 841 (1997).
⁵I. Hotovy, J. Huran, D. Buc, and R. Srnanek, *Vacuum* **50**, 45 (1998).
⁶J. Bantista, *IEEE Trans. Magn.* **21**, 640 (1985).
⁷J.-C. Villegier, B. Delaet, Ph. Feautrier, L. Frey, C. Delacour, and V. Bouchiat, *J. Phys.: Conf. Ser.* **43**, 1373 (2006).
⁸J. B. Walker, *IEEE Trans. Appl.* **25**, 885 (1977).
⁹I. S. Beloborodov, A. V. Lopatin, V. M. Vinokur, and K. B. Efetov, *Rev. Mod. Phys.* **79**, 469 (2007).
¹⁰B. I. Belevtsev, *Usp. Fiz. Nauk* **160**, 65 (1990).
¹¹V. F. Gantmakher and V. T. Dolgoplov, *Usp. Fiz. Nauk* **180**, 1 (2010).
¹²R. W. Simon, B. J. Dalrymple, D. Van. Vechten, W. W. Fuller, and S. A. Wolf, *Phys. Rev. B* **36**, 1962 (1987).
¹³R. Fazio and H. S. J. van der Zant, *Phys. Rep.* **355**, 235 (2001).
¹⁴A. M. Glukhov, O. G. Turutanov, V. I. Shnyrkov, and A. N. Omel'yanchuk, *Fiz. Nizk. Temp.* **32**, 1477 (2006) [*Low Temp. Phys.* **32**, 1123 (2006)].
¹⁵A. M. Glukhov, A. S. Pokhila, I. M. Dmitrenko, A. E. Kolinko, and A. P. Panchevka, *Physica B* **240**, 242 (1997).
¹⁶B. Kościelska, L. Murawski, and L. Wicikowski, *Mat. Sci.-Poland* **23**, 93 (2005).
¹⁷Yu. Yeshurun and A. P. Malozemoff, *Phys. Rev. Lett.* **60**, 2202 (1988); A. P. Malozemoff, Yu. Yeshurun, L. Krusin-Elbaum, T. K. Worthington, D. C. Cronmeyer, T. Dinger, T. R. Foltzberg, T. R. McGuire, and P. H. Kes, *High-Temperature Superconductivity*, World Scientific, Singapore, vol. 9, p. 112 (1988).
¹⁸P. W. Anderson, *Phys. Rev. Lett.* **9**, 309 (1962); Y. B. Kim, *Rev. Mod. Phys.* **36**, 39 (1964).
¹⁹D. H. Kim, K. E. Gray, R. T. Kampwirth, K. C. Woo, D. M. McKay, and J. Stein, *Phys. Rev. B* **41**, 11642 (1990).
²⁰M. P. A. Fisher, *Phys. Rev. Lett.* **65**, 923 (1990).
²¹V. M. Galitski and A. I. Larkin, *Phys. Rev. B* **63**, 174506 (2001).
²²Y. Strelniker, A. Frydman, and S. Havlin, *Phys. Rev. B* **76**, 224528 (2007).

Translated by D. H. McNeill